Available online at www.sciencedirect.com
SCIENCE DIRECT®
Journal of Power Sources 126 (2004) 229–235
JOURNAL OF POWER SOURCES
www.elsevier.com/locate/jpowsour

Electrocatalytic activities of $REMn_2O_5$ (RE = Dy, Ho, Er, Tm, Yb, and Lu) and $Er_{0.76}Zr_{0.11}Ca_{0.13}Mn_2O_5$ for oxygen reduction in alkaline solution

Neng Li*, Xiang Xu, Dan Luo, Yishi Wu, Shijie Li, Bingxiog Lin

Institute of physical Chemistry Peking University, Beijing 100871, China

Received 5 September 2002; received in revised form 13 August 2003; accepted 25 August 2003

Abstract

A series of complex oxides $REMn_2O_5$ (RE = Dy, Ho, Er, Tm, Yb, and Lu) and $Er_{0.76}Zr_{0.11}Ca_{0.13}Mn_2O_5$ with large specific areas and nanoscale grain sizes were prepared by an improved amorphous citric precursor method (IACP). Their electrocatalytic performances were characterized by the polarization curves of gas diffusion electrodes employing the oxides. The measurement of polarization curves indicated that the $REMn_2O_5$ containing different rare earth showed a obviously different electrocatalytic performances for oxygen reduction reaction, being the order Tm > Er > Ho > Dy > Lu > Yb. Temperature-programmed reduction (TPR) analysis revealed that the $REMn_2O_5$ containing different rare earth showed a significantly different oxygen contents and TPR peak temperatures. Their catalytic activities depended on both the oxygen contents and TPR peak temperatures. These two factors play a plus and a minus role respectively.

Keywords: $REMn_2O_5$; Electrocatalysis; Oxygen reduction

1. Introduction

Rare-earth dimanganese oxides $REMn_2O_5$, (RE = Dy, Ho, Er, Tm, Yb, and Lu) were first synthesized by Quezel-Ambrunaz et al. [1]. The crystal structures [2–4] have been investigated. Ten years ago, single crystals of $NdMn_2O_5$ with a good quality were prepared by Euzen et al. [5]. According to them, $NdMn_2O_5$ has the orthorhombic structure in the space group *Pbam* (D_{2h}^9). There are four $REMn_2O_5$ per until cell and two independent Mn atoms. Their structure consist of Mn^{4+} octahedral [MnO_6] in infinite chains parallel to the axis linked through Mn^{3+} tetragonal pyramid [Mn_2O_5] and RE square-anti-prismatic polyhedron [REO_8].

The magnetic structure at low temperature [6–9], dielectric properties [10] and phase stability [11] of $REMn_2O_5$ have been investigated. The catalytic activity for electrochemical reduction of oxygen was not reported. The perovskite-type manganites, $REMnO_3$ were examined for their electocatalytic activities to reduce oxygen in alkaline solution by Hyodo et al. [12]. They revealed that the catalytic activity differed significantly with a change in RE, but the reason for this is not clear. In this paper, a study of electrocatalytic activities of $REMn_2O_5$ (RE = Dy; Ho, Er, Tm, Yb, and Lu) oxides is described.

2. Experimental

2.1. Preparation and characterization of the catalysts

The formation of $REMn_2O_5$ was difficult by the usual ceramic method. The formation of YMn_2O_5 could be realized only by the nitrate solution [13]. Satoh et al. obtained $REMn_2O_5$ phase by using two methods [11]: (1) by heating the nitrate solution at 1373 K; and (2) by the decomposition of mixed 2-ethylhexanoates of rare earth and manganese at 1273 K. In our experiment, IACP method [14] was tried to prepare $REMn_2O_5$ (RE = Dy, Ho, Er, Tm, Yb, and Lu) phases. RE_2O_3 (Dy_2O_3, Ho_2O_3, Er_2O_3, 99.9% in purity; Tm_2O_3, Yb_2O_3, Lu_2O_3, 99.99% in purity) and $Mn(NO_3)_2$ (A.R. $Mn(NO_3)_2$ 50% solution) were used as starting materials. RE_2O_3 was heated at 800 °C in air for 4 h and $Mn(NO_3)_2$ solution was analyzed by EDTA complexometric titration. After such pretreatment, RE_2O_3 in an appropriate ratio was dissolved into HNO_3 solution; then $Mn(NO_3)_2$ solution in an appropriate ratio was added. The citric acid (A.R.), molar ratio of RE^{3+} and Mn^{2+} to citric acid was

* Corresponding author. Fax: +86-10-62754139.
E-mail address: lineng@pku.edu.cn (N. Li).

0378-7753/$ – see front matter © 2003 Elsevier B.V. All rights reserved.
doi:10.1016/j.jpowsour.2003.08.027

(1:1), was also added. To prepare $Er_{0.76}Zr_{0.11}Ca_{0.13}Mn_2O_5$ oxide $ZrO(NO_3)_2{\cdot}2H_2O$ (A.R.) and $Ca(NO_3)_2$ (A.R.) were used as starting materials. $ZrO(NO_3)_2{\cdot}2H_2O$ were analyzed by gravimetric analysis and $Ca(NO_3)_2$ by EDTA complexometric titration respectively. The solution and citric acid were mixed with sufficient agitating and left overnight, then a certain amount of carbon black (cabot VXC-72) with a overall surface area of 254 $m^2\ g^{-1}$ was added to prevent agglomeration among the particles of the oxides. The mixture was dried at 95 °C, ground into fine powder, and decomposed at 200 °C in air for 2 h; then the samples were heated at 700 °C 5 h and 800 °C 5 h in the same atmosphere, and cooled slowly with the furnace to room temperature.

The lattice parameters and an average grain sizes were examined by powder X-ray diffraction (Rigaku D/max-rA, Cu Kα). A graphite diffracted beam monochromator was used to improve signal to noise characteristics. BET-surface area of the samples were obtained from nitrogen absorption isotherms (ASAP 2010 Micromeritics) on degassed at liquid nitrogen temperature.

The temperature-programmed reduction (TPR) analysis was used to examine the oxygen contents of the oxides. Each sample (40 mg), after being mounted in a silica-glass reactor, was preheated at 300 °C under nitrogen with a flowing rate 30 ml/min for 1 h, followed by cooled to room temperature in the same atmosphere. After substitution of atmosphere with the gas mixture containing 5% (v/v) H_2 in nitrogen with a flowing rate 30 ml/min, the sample was heated at a constant rate of 10 °C/min. The hydrogen left, after dried by anhydrous magnesium perchlorate $Mg(ClO_4)_2$, was monitored with a thermal conductivity detector. The phases of the reduced powder were identified by powder X-ray diffraction.

2.2. Preparation of electrode and electrochemical measurement

A gas diffusion layer and a reaction layer formed the gas diffusion electrode. The gas diffusion layer consisted of ethyne black (70 wt.%), PTFE (30 wt.%) and an embedded nickel mesh (80 mesh, current collector). The reaction layer consisted of oxides catalyst (25 wt.%), carbon black (Cabot VXC-72, 254 $m^2\ g^{-1}$, 60 wt.%) and PTFE (15 wt.%). To prepare the layers, first ethyne black or a carbon-oxide mixture was suspended in water containing a dispersant Triton X-100 (TX-100/water = 1:500) was added and mixed. The suspension was evaporated and dried for 2 h at 100 °C. The dried gas diffusion layer or the reaction layer was heated for 3 h in N_2 at 300 °C or 280 °C. The cakes obtained were pulverized into fine powders. The powders were cool-Pressed onto the Ni mesh to make a stacking of the layers. Then the assembly was sintered at 350 °C for 15 min, and hot-pressed for 20 s under 6 MPa, into a laminated sheet with 18 mm diameter and about 0.5 mm thickness. The polarization curves, referred to a Hg/HgO electrode, were measured in 7 M KOH at (20 ± 3) °C under an oxygen flow of 100 ml/min. To compare the electrocatalytic activities of different materials in composition, five electrodes of the same material were prepared and measured.

3. Results and discussion

The $REMn_2O_5$ (RE = Dy, Ho, Er, Tm, Yb, and Lu) are all brown fine powder. Their X-ray diffraction patterns are given in Fig. 1. Their lattice parameters, average grain sizes and specific surface areas are listed in Table 1. The

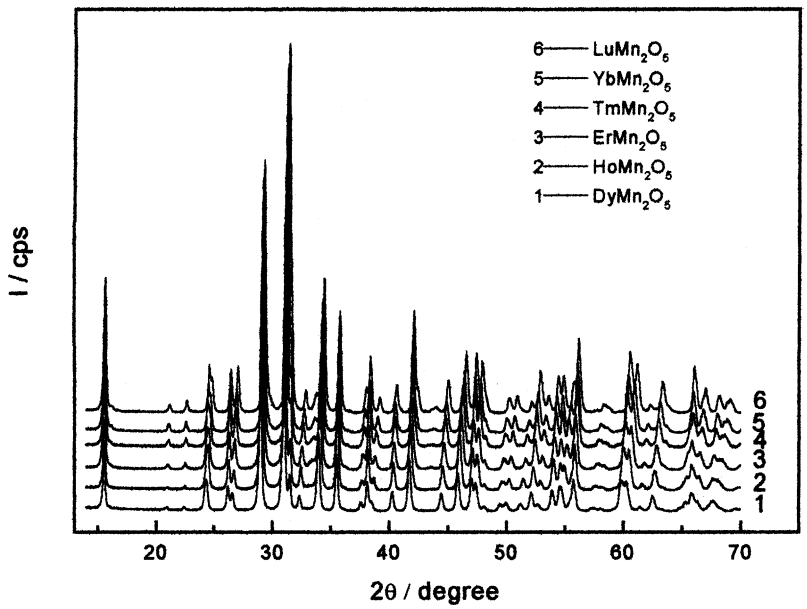

Fig. 1. X-ray diffraction patterns of the $REMn_2O_5$ (Re = Dy, Ho, Er, Tm, Yb, and Lu) oxides synthesized at 700 °C 5 h and 800 °C 5 h in air.

Table 1
Lattice parameters (a, b, and c), cell volume (v), average grain sizes ($D_{(122)}$), specific surface areas (S) of REM_2O_5 (RE = Dy, Ho, Er, Tm, Yb, and Lu) oxides

Specimen	a (nm)	b (nm)	c (nm)	v (nm^3)	$D_{(122)}$ (nm)	S (m^2 g^{-1})
$DyMn_2O_5$	0.7291	0.8486	0.5672	0.3509	64	19.6
$HoMn_2O_5$	0.7261	0.8466	0.5670	0.3485	65	16.9
$ErMn_2O_5$	0.7234	0.8445	0.5665	0.3461	50	20.8
$TmMi_2O_5$	0.7218	0.8428	0.5658	0.3442	65	18.1
$YbMn_2O_5$	0.7192	0.8404	0.5654	0.3417	75	17.3
$LuMn_2O_5$	0.7166	0.8385	0.5634	0.3397	120	17.9

lattice parameters are in good agreements with [2,3,11]. As seen in the Table 1, all the samples synthesized by IACP method have a similar specific surface area and nanoscale grain size. Compared with [11,13], in this paper $REMn_2O_5$ phases could be obtained by IACP method at a relative lower (200–300 °C) temperature. It is very helpful to prepare the catalyst with a large surface area.

The $REMn_2O_5$ oxide containing transition metal Mn, in general, the valence state of Mn can be modified by doping of the RE cation site with other cation having different valences. In the beginning we tried to substitute Er with the cation Sr^{2+}, or Ca^{2+} to prepare $Er_{1-x}M_xMn_2O_5$, however, we cannot obtain any single-phase compounds. In some time later, we found a reference paper in JCPDS 46–0422, which reported Ivanov and Zhurov [16] prepared a single crystal with a formula $Y_{0.76}Zr_{0.11}Ca_{0.13}Mn_2O_5$. By following this idea, $Er_{0.76}Zr_{0.11}Ca_{0.13}Mn_2O_5$ were synthesized in IACP method at 700 °C 5 h and 800 °C 5 h. As seen in Fig. 2, its XRD pattern was almost the same with $ErMn_2O_5$. Its lattice parameter, average grain size and specific surface area are listed in Table 2. It seems that the valence of manganese in $Er_{0.76}Zr_{0.11}Ca_{0.13}Mn_2O_5$ is lightly higher than that in the $ErMn_2O_5$ when the ratio O/Mn is exactly 2.5 for both compounds.

Figs. 3 and 4 showed the polarization curves of electrodes loaded with $REMn_2O_5$ or $Er_{0.76}Zr_{0.11}Ca_{0.13}Mn_2O_5$ catalysts respectively. The curve of pure carbon (Cabot VXC-72) electrode was also shown for comparison. As seen in Figs. 3–4 all catalyst-loaded electrodes performed much better than the pure carbon electrode. In this paper, polarization experiments revealed that the $REMn_2O_5$ containing different rate earth showed a significantly different electrocatalytic activities for oxygen reduction reaction, being in the order Tm > Er > Ho > Dy > Lu > Yb. Why do not this order coincide with the atomic numbers of Dy, Ho, Er, Tm, Yb, and Lu? Fig. 4 showed that electrocatalytic activity of $Er_{0.76}Zr_{0.11}Ca_{0.13}Mn_2O_5$ was lower than its parent compound $ErMn_2O_5$ which is unexpected.

In order to account for these variations in catalytic activities of the oxides, it is essential to examine the oxygen content of the oxides for the activity depends on the

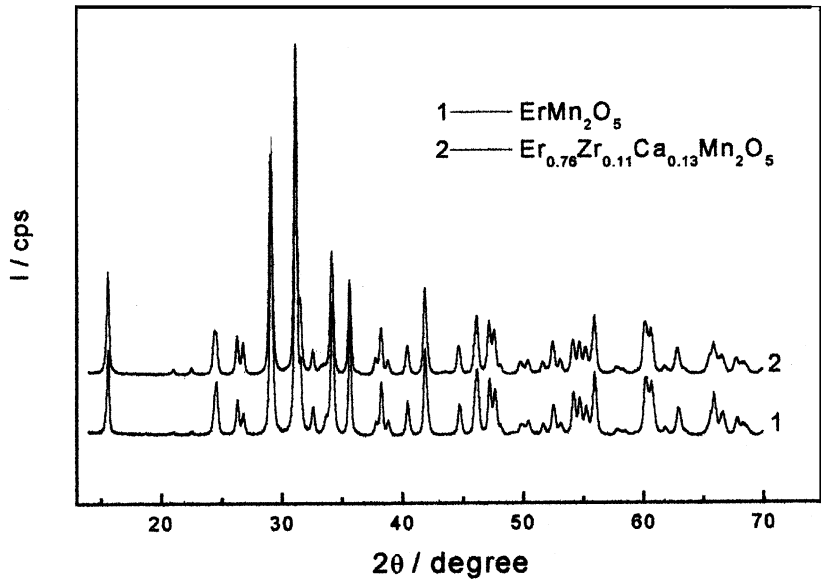

Fig. 2. X-ray diffraction patterns of the samples: (1) $ErMn_2O_5$ and (2) $Er_{0.76}Zr_{0.11}Ca_{0.13}Mn_2O_5$.

Table 2
Lattice parameters (a, b, and c), cell volume (v), average graim sizes ($D_{(122)}$), specific surface areas (S) of $ErMn_2O_5$ and $Er_{0.76}Zr_{0.11}Ca_{0.13}Mn_2O_5$

Specimen	a (nm)	b (nm)	c (nm)	v (nm^3)	$D_{(122)}$ (nm)	S (m^2 g^{-1})
$ErMn_2O_5$	0.7234	0.8445	0.5665	0.3461	50	20.8
$Er_{0.76}Zr_{0.11}Ca_{0.13}Mn_2O_5$	0.7232	0.8429	0.5665	0.3453	50	20.8

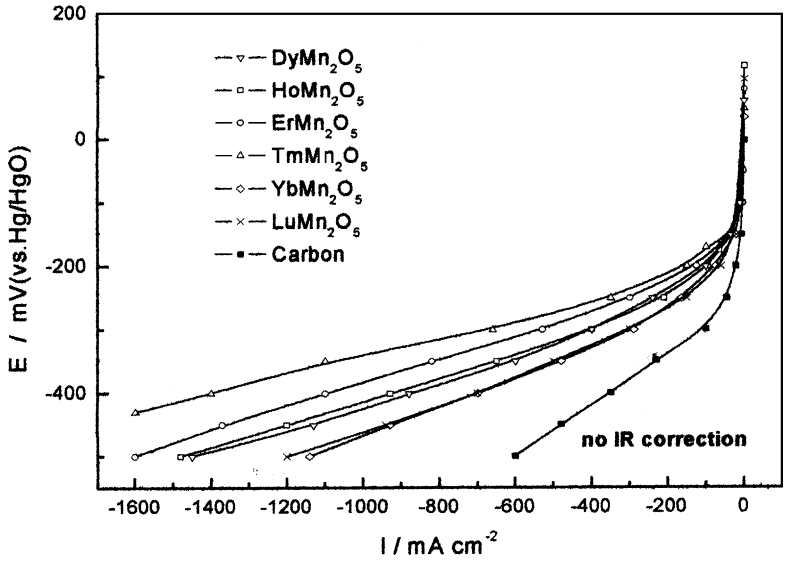

Fig. 3. Cathodic polarization curves of gas diffusion electrodes loaded with 25 wt.% $REMn_2O_5$ catalysts.

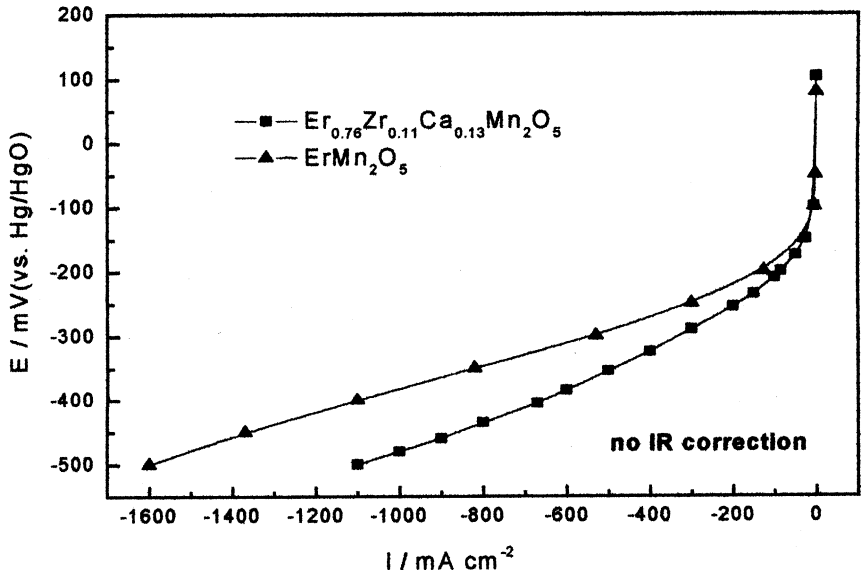

Fig. 4. Cathodic polarization curves of gas diffusion electrodes loaded with 25 wt.% $Er_{0.76}Zr_{0.11}Ca_{0.13}Mn_2O_5$ or $ErMn_2O_5$ catalyst.

oxygen content. Zhang et al. [15] investigated the variations in catalytic activities with perovskite-type oxide composition by a temperature-programmed desorption (TPD) technique. Wu et al. [17] examined the effect of oxygen content on electrocatalysis of $La_{0.6}Ca_{0.4}CoO_{3-x}$ by a temperature-programmed reduction technique. Regarding references above, we used TPR technique in this study. Figs. 5–7 show the temperature-programmed reduction spectra of the oxides. TPR analysis given only one reduction peak at different peak temperature which depended on the rare earth. The results were summarized in Table 3. As shown in the Table 3, the $REMn_2O_5$ containing different rare earth showed significant variations primarily in the peak area and the peak tempera-

Table 3
The results from TPR analysis

Specimen	Peak area (mV s)	Peak height (mV)	Peak temperature (°C)
$TmMn_2O_5$	13020	28.2	508
$ErMn_2O_5$	6597	20.2	506
$LuMn_2O_5$	5265	16.2	507
$DyMn_2O_5$	10664	24.6	524
$HoMn_2O_5$	8476	21.3	518
$YbMn_2O_5$	8263	21.6	511
$Er_{0.76}Zr_{0.11}Ca_{0.13}Mn_2O_5$	11930	22.8	518

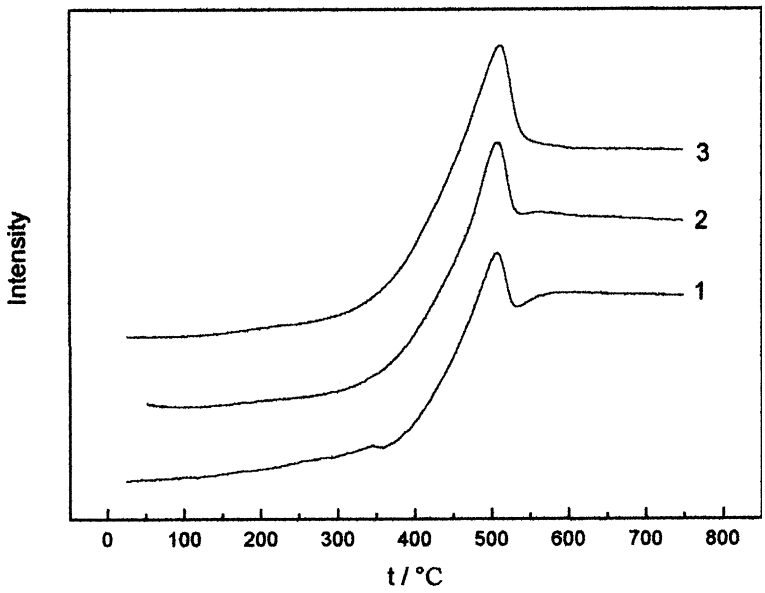

Fig. 5. Temperature-programmed reduction (TPR) spectra of the following samples: (1) $LuMn_2O_5$, (2) $ErMn_2O_5$, and (3) $TmMn_2O_5$.

ture associated with reduction of Mn cation. In Fig. 8, XRD patterns of three reduced samples (cooled to room temperature in N_2 atmosphere) showed the presence of RE_2O_3 (JCPDS, Tm_2O_3: 10–350, Lu_2O_3: 12–728, Er_2O_3: 8–50) and MnO (JCPDS, 7–230), the oxides of Zr and Ca could not he observed since they were in a rather low content. It is concluded that the observed reduction peaks were due to the reduction of Mn cation from about +3.5 valence to +2 valence. The results from XRD and TPR analysis, which characterized mainly the bulk properties of the powders, indicated the oxygen content of each $REMn_2O_5$ oxide. Based on Table 3, we obtain a variations of activities with oxygen contents in the order of Tm > Dy > Ho > Yb > Er > Lu. Among them, the order Tm > Er > Lu is coincided with the order obtained from polarization experiments, but the order of Dy, Ho, and Yb was different. So, the peak temperatures may also take a respective effect. It is concluded that electrocatalytic activities of the $REMn_2O_5$ oxides were affected by their oxygen contents and TPR peak temperatures. These two factors play a plus and a minus role respectively. TPR analysis indicated that $Er_{0.76}Zr_{0.11}Ca_{0.13}Mn_2O_5$ had both much higher oxygen content and peak temperature than its parent $ErMn_2O_5$. It showed lower activity than its parent because its peak temperature was apparently rise. Satoh et al. investigated the thermodynamic stabilities of $REMn_2O_5$ phases. They reported that $DyMn_2O_5$ and $HoMn_2O_5$ had the maximum

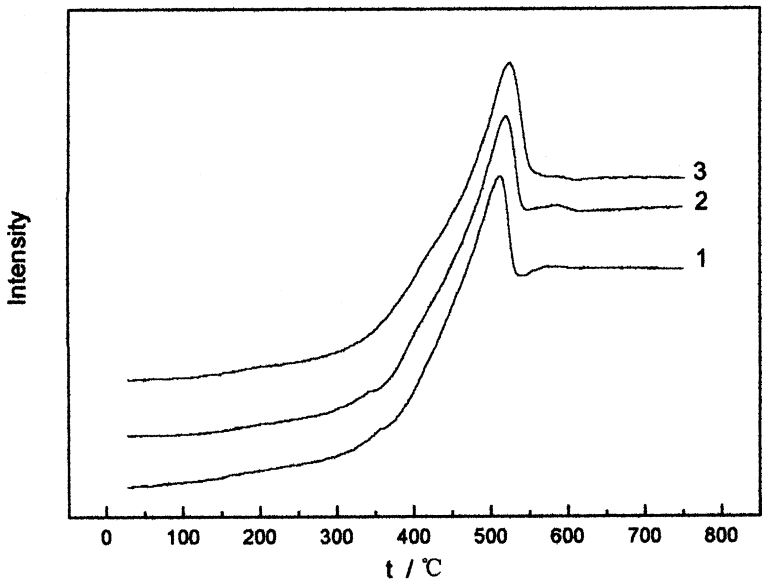

Fig. 6. Temperature-programmed reduction (TPR) spectra of the following samples: (1) $YbMn_2O_5$, (2) $HoMn_2O_5$, and (3) $DyMn_2O_5$.

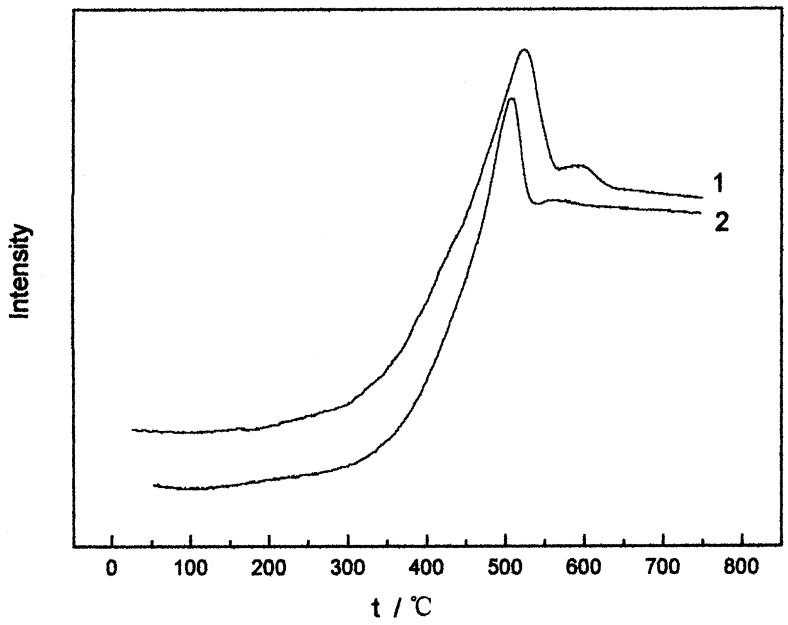

Fig. 7. Temperatre-programmed reduction (TPR) spectra of the samples: (1) $Er_{0.76}Zr_{0.11}Ca_{0.13}Mn_2O_5$ and (2) $ErMn_2O_5$.

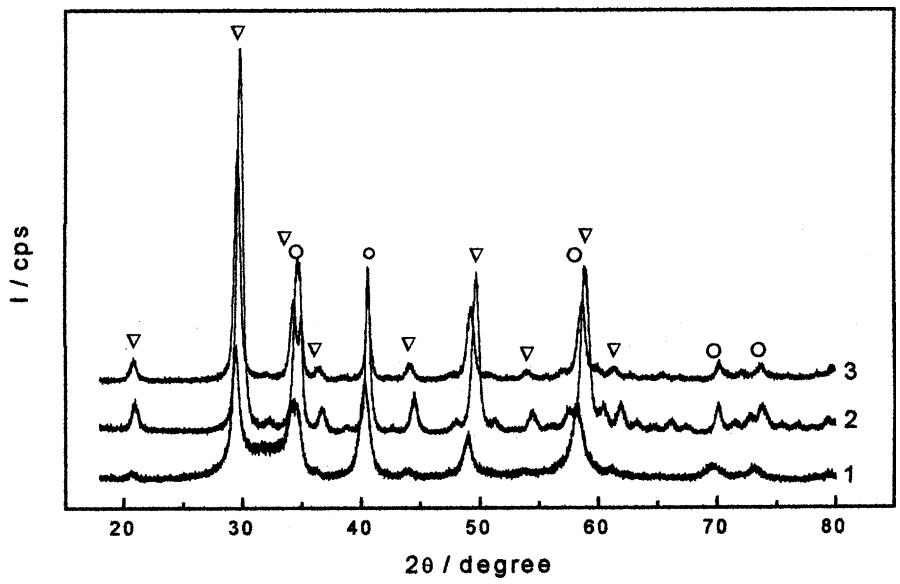

Fig. 8. X-ray diffraction patterns of the reduced powders of the followmg samples: (1) $Er_{0.76}Zr_{0.11}Ca_{0.13}Mn_2O_5$, (2) $LuMn_2O_5$, and (3) $TmMn_2O_5$. (▽) RE_2O_3 (JCPDS, Tm_2O_3: 10–350, Lu_2O_3: l2–728, Er_2O_3: 8–50); (○) MnO (JCPDS, 7–230).

temperature for stability in air [11]. In this study, TPR analysis also revealed that these two compounds had the maximum peak temperature. It seems that the high TPR peak temperature corresponds to the high thermodynamic stability of the oxides. So, the more stable compound has the lower electrocatalytic activity. Based on TPR analysis, we suppose that Dy, Ho, and Yb affect stronger than the Tm, Er, and Lu in the $REMn_2O_5$ phases on the Mn–O bond strength. Therefore the data of thermodynamic stability and TPR peak temperature of the $REMn_2O_5$ phases are an useful information for evaluating their catalytic activities.

4. Summary and conclusion

The IACP method presented here is an useful way of preparing $REMn_2O_5$ (RE = Dy, Ho, Er, Tm, Yb, and Lu) and $Er_{0.76}Zr_{0.11}Ca_{0.13}Mn_2O_5$ oxides at relatively lower temperature. It permits the possibility to decrease the reaction time and obtain a number of oxides, each with a large specific surface area and a nanoscale grain size.

Polarization experiments using gas diffusion electrodes revealed that $REMn_2O_5$ containing different rare earth showed significantly different electrocatalytic performances

for oxygen reduction, being in the order Tm > Er > Ho > Dy > Lu > Yb.

TPR analysis indicated that $REMn_2O_5$ containing different rare earth showed a significantly different oxygen content and peak temperature. Their electrocatalytic performances depended on both the oxygen content and the peak temperature. These two factors play a plus and a minus role respectively.

References

[1] S. Quezel-Ambrunaz, E.F. Bertaut, G. Buisson, C. R. Acad. Sci. 258 (1964) 3025.
[2] E.F. Bertaut, G. Buisson, A. Durif, A. Mareschal, M.C. Montmory, S. Quezel-Ambrunaz, Bull. Soc. Chim. France (1965) 1132.
[3] S.C. Abrahams, J.L. Bernstein, J. Chem. Phys. 46 (1967) 3776.
[4] B.M. Wanklyn, J. Mater. Sci. A 7 (1973) 813.
[5] P. Euzen, P. Leone, C. Gueho, P. Palvadeau, Acta Crystallogr. C 49 (1993) 1875.
[6] G. Buisson, J. Phys. Chem. Solids 31 (1970) 1171.
[7] I. Yaeger, Mater. Res. Bull. 13 (1978) 819.
[8] G. Buisson, Phys. Status Solidi A 17 (1973) 191.
[9] P. P gardner, C. Wilkinson, J.B. Forsyth, B.M. Wanklyn, J. Phys. C 21 (1988) 5653.
[10] V.A. Sanina, L.M. Sapozhnikova, E.I. Golovenchits, N. V Morozov, Fiz. Tverd. Tela (Leningrad) 30 (1988) 3015.
[11] H. Satoh, S. Suzuki, K. Yamamoto, N. Kamegashira, J. Alloys Compd. 234 (1996) 1.
[12] T. Hyodo, M. Hayashi, N. Miura, N. Yamazoe, J. E1ectrochem. Soc. 143 (1996) L266.
[13] G. Buisson, in: J.P. Suchet (Ed.), Croissance de Composes Mineraux Monocristallins, Masson, Paris, 1969.
[14] N. Li, X. Yan, W. Zhang, B. Lin, J. Power Sources 74 (1998) 255.
[15] H.M. Zhang, Y. Shimizu, Y. Teraoka, N. Miura, N. Yamazoe, J. Catal. 121 (1990) 432.
[16] S. Ivanov, V. Zhurov, JCPDS 46–0422.
[17] N.-L. Wu, W.-R. Liu, S.-J. Su, Electrochim. Acta 48 (2003) 1567.